

Entanglement distillation by Hong-Ou-Mandel interference with orbital angular momentum states

Cite as: APL Photonics 4, 016103 (2019); <https://doi.org/10.1063/1.5079970>

Submitted: 05 November 2018 . Accepted: 04 January 2019 . Published Online: 25 January 2019

B. Ndagano , and A. Forbes 

COLLECTIONS

 This paper was selected as an Editor's Pick



View Online



Export Citation



CrossMark

ARTICLES YOU MAY BE INTERESTED IN

[High temperature, experimental thermal memory based on optical resonances in photonic crystal slabs](#)


APL Photonics 4, 010804 (2019); <https://doi.org/10.1063/1.5049174>

[Enhanced magneto-optical effects in hybrid Ni-Si metasurfaces](#)

APL Photonics 4, 016102 (2019); <https://doi.org/10.1063/1.5066307>

[Nonlinear propagation equations in fibers with multiple modes—Transitions between representation bases](#)

APL Photonics 4, 022806 (2019); <https://doi.org/10.1063/1.5084118>



AMERICAN ELEMENTS

THE ADVANCED MATERIALS MANUFACTURER®

additive manufacturing epitaxial crystal growth cerium oxide polishing powder silver nanoparticles sputtering targets III-IV semiconductors CVD precursors europium phosphors

deposition slugs OLED Lighting spintronics solar energy osmium nanoribbons thin films chalcogenides AuNPs

GDC Li-ion battery electrolytes 99.999% ruthenium spheres

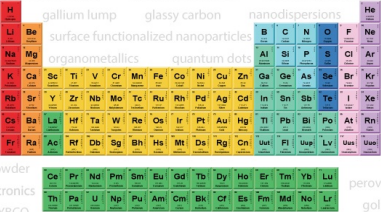
endohedral fullerenes copper nanoparticles diamond micropowder CIGS MBE grade materials palladium catalysts flexible electronics

beta-barium borate borosilicate glass dysprosium pellets YBCO

pyrolytic graphite 3d graphene foam indium tin oxide mesoporous silica

raman substrates sapphire windows tungsten carbide InGaAs

barium fluoride carbon nanotubes lithium niobate scandium powder



gallium lump glassy carbon nanodispersions He

surface functionalized nanoparticle: organometallics quantum dot Al Si P S Cl Ar

perovskite crystals yttrium iron garnet alternative energy h-BN

rhodium sponge fiber optics beamsplitters infrared dyes zeolites

fused quartz metallocenes platinum ink buckyballs Ti-6Al-4V

inAs wafers laser crystals ultra high purity materials MOFs

rare earth metals photovoltaics refractory metals MOCVD

superconductors transparent ceramics ultra high purity silicon

American Elements opens up a world of possibilities so you can **Now Invent!**

Over 15,000 certified high purity laboratory chemicals, metals, & advanced materials and a state-of-the-art Research Center. Printable GHS-compliant Safety Data Sheets. Thousands of new products. And much more. All on a secure multi-language "Mobile Responsive" platform.

www.americanelements.com

Now Invent.™
The Next Generation of Material Science Catalogs



Entanglement distillation by Hong-Ou-Mandel interference with orbital angular momentum states

Cite as: APL Photon. 4, 016103 (2019); doi: 10.1063/1.5079970
Submitted: 5 November 2018 • Accepted: 4 January 2019 •
Published Online: 25 January 2019



B. Ndagano^{a)}  and A. Forbes 

AFFILIATIONS

School of Physics, University of the Witwatersrand, Private Bag 3, Wits 2050, South Africa

^{a)}Electronic mail: nibienvenu@gmail.com

ABSTRACT

Entanglement is an invaluable resource to various quantum communication, metrology, and computing processes. In particular, spatial entanglement has become topical, owing to its wider Hilbert space that allows photons to carry more information. However, spatial entanglement is susceptible to decay in the presence of external perturbations such as atmospheric turbulence. Here we show theoretically and experimentally that in a weak turbulence regime, maximally entangled states can be distilled through quantum interference. We generated entangled photons by spontaneous parametric down-conversion, with one photon in the entangled pairs being sent through a turbulent channel. We recombined the paths of the two photons at a beam-splitter in a Hong-Ou-Mandel interference setup and measured in coincidence, using spatial filters, the spatial correlations between photons in the output ports of the beam-splitter. We performed a state tomography and show that, from an ensemble of pure states with very low levels of entanglement, we distil entangled states with fidelities $F \geq 0.90$ with respect to the singlet Bell state.

© 2019 Author(s). All article content, except where otherwise noted, is licensed under a Creative Commons Attribution (CC BY) license (<http://creativecommons.org/licenses/by/4.0/>). <https://doi.org/10.1063/1.5079970>

I. INTRODUCTION

Generating, manipulating, and sharing quantum states with maximal levels of entanglement are crucial steps to realising quantum processes such as quantum key distribution, teleportation, metrology, and computation.¹⁻¹¹ In this quest, realising entanglement in different degrees of freedom has opened avenues beyond the two-level quantum bit (qubit). Spatial modes, particularly those carrying orbital angular momentum (OAM), allow one to exploit the spatial properties of photons to realise high-dimensional entanglement.¹²⁻¹⁵ However, correlations between entangled spatial modes are adversely affected by external factors such as atmospheric turbulence.¹⁶⁻²² These perturbations reduce the degree of entanglement and, consequently, the fidelity of the quantum process implemented. This constitutes a major hindrance in processes where maximally entangled states are required. Methods to mitigate the effects of turbulence on

spatial modes have been proposed, with some notable ones including increasing the separation in mode space to reduce cross talk²³ and performing a coordinate transformation on one of the entangled photons to cancel out antisymmetric contributions of the turbulence.²⁴

Through entanglement concentration or distillation, one can sift, from an ensemble, a fraction of states with a higher degree of entanglement.²⁵⁻²⁷ In the special case of pure states, entanglement distillation can be realised in two ways. The first is through Procrustean filtering, where local operations on the entangled pair are performed in order to control the probability amplitudes of the post-selected states. Naturally, this requires prior knowledge of the quantum states before filtering. First demonstrated with polarisation states,²⁸ this technique has been extended to spatial modes in higher dimensions.¹⁵ The second method is the Schmidt projection and, unlike the first, can be applied to an unknown quantum state. Although efficient for large ensembles of entangled

pairs, this scheme is impractical as it requires collective measurements to be performed on the ensemble.²⁵ Alternative schemes to realise the Schmidt projection have been proposed to circumvent the requirement for collective measurements, many of which involve ancillary photons (pairs).²⁹⁻³³

In the present work, we address the issue of entanglement distillation on an ensemble of OAM entangled photons generated by spontaneous parametric down-conversion (SPDC) and perturbed by a one-sided weak turbulent channel. One of the photons in the entangled pair propagates through the turbulence, leading to a unitary scattering in a higher dimensional OAM space. As a result of post-selection on a particular OAM subspace, one measures a decay of the degree of entanglement despite the unitary nature of the channel operator. To distil entanglement, we interfere the non-maximally entangled photons in a Hong-Ou-Mandel (HOM) configuration.^{34,35} It has been shown that the HOM interference can be exploited to implement a filter for Bell states according to their intrinsic symmetry.³⁶⁻³⁸ By performing a state tomography of the quantum states after implementing the HOM filter, we obtained distilled entangled singlet states with fidelity $F \geq 0.90$, up from as low as $F = 0.03$.

II. THEORY

Consider the OAM entangled two-photon state $|\Psi_{\ell}^{-}\rangle$ expressed as follows:

$$|\Psi_{\ell}^{\pm}\rangle = \frac{1}{\sqrt{2}}(|\ell\rangle_A |-\ell\rangle_B \pm |-\ell\rangle_A |\ell\rangle_B), \quad (1)$$

where the subscripts A and B label each of the photons in the entangled pair carrying $\ell\hbar$ quanta of OAM. Photon A is allowed to propagate through a turbulent channel that is unitary,

causing a scattering of OAM states,

$$|\ell\rangle \xrightarrow{\text{turbulence}} \sum_{\ell'} c_{\ell-\ell'} |\ell'\rangle, \quad (2)$$

where $\sum_{\ell'} |c_{\ell-\ell'}|^2 = 1$. While the scattering certainly leads to the formation of higher-dimensional correlations, we will restrict the problem to a qubit subspace by projecting on the initial OAM state space; that is, we will consider the terms with $\ell' = \pm\ell$ in Eq. (2). The perturbed qubit state after turbulence then becomes

$$|\Psi_{\ell}\rangle = \frac{1}{\sqrt{2}} \left(c_0 |\ell\rangle_A |-\ell\rangle_B - c_0 |-\ell\rangle_A |\ell\rangle_B + c_{2\ell} |-\ell\rangle_A |-\ell\rangle_B - c_{-2\ell} |\ell\rangle_A |\ell\rangle_B \right). \quad (3)$$

It is useful at this point to express $|\Psi_{\ell}\rangle$ in the Bell basis. This can be done by realising that the last two terms in Eq. (3) correspond to a state on a two-photon OAM Bloch sphere,³⁹ where the poles are the Bell states $|\Phi_{\ell}^{+}\rangle$ and $|\Phi_{\ell}^{-}\rangle$, expressed as follows:

$$|\Phi_{\ell}^{\pm}\rangle = \frac{1}{\sqrt{2}} (|-\ell\rangle_A |-\ell\rangle_B \pm |\ell\rangle_A |\ell\rangle_B). \quad (4)$$

One then rewrites Eq. (3), the Bell basis, as follows:

$$|\Psi_{\ell}\rangle = c_0 |\Psi_{\ell}^{-}\rangle + c_{2\ell}^{+} |\Phi_{\ell}^{+}\rangle + c_{2\ell}^{-} |\Phi_{\ell}^{-}\rangle, \quad (5)$$

where $c_{2\ell}^{\pm} = \langle \Phi_{\ell}^{\pm} | \Psi_{\ell} \rangle$.

After the turbulent channel, the photons enter a Hong-Ou-Mandel filter, as shown in Fig. 1(a). The aim of this filter is to distil the singlet state $|\Psi_{\ell}^{-}\rangle$ from the perturbed state $|\Psi_{\ell}\rangle$. The layout of the filter is shown as the inset in Fig. 1(a) and consists of two mirrors and a 50:50 beam-splitter (BS).

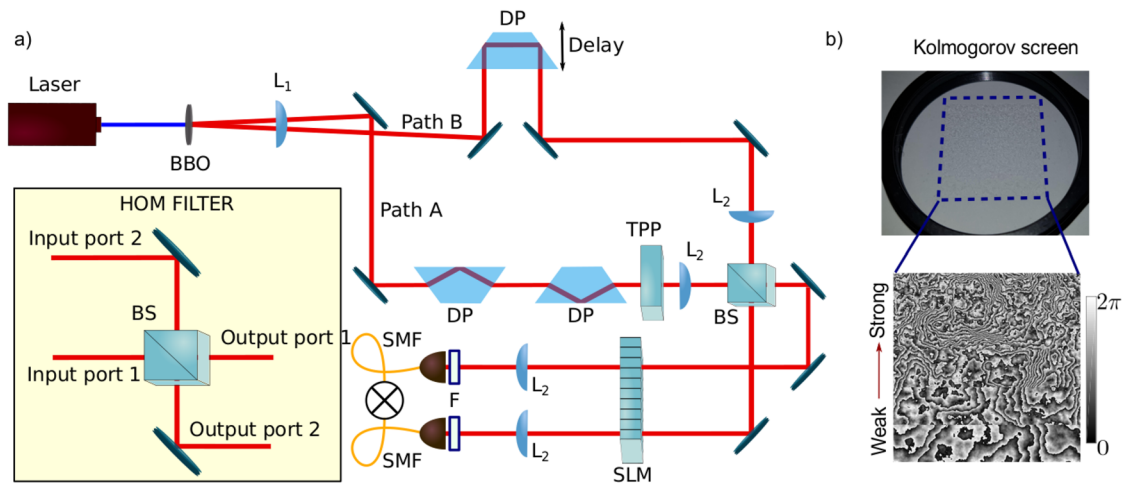


FIG. 1. Experimental setup for entanglement distillation. (a) By pumping a 3-mm thick, non-linear type-I BBO crystal with a 355 nm laser, we produced, through SPDC, pairs of entangled photons with wavelength 710 nm. The photons are sent down two paths, one containing a delay line and another with two Dove prisms (DP) to manipulate the SPDC state symmetry. A turbulence phase plate (TPP) in path A perturbs the state before the photon paths are recombined at a 50:50 beam-splitter (BS). Lenses L_1 and L_2 with focal lengths $f_1 = 100$ mm and $f_2 = 750$ mm, respectively, relay the plane of the BBO crystal onto the spatial light modulator (SLM). The two photons are probed using digital holograms encoded on the SLM, passed through 10 nm bandpass filters (F), and then coupled to single mode fibres (SMF). (b) shows the range of phase fluctuations across the turbulence phase plate.

A general entangled state $|\Psi\rangle = (|l_1\rangle_A |-\ell_2\rangle_B \pm |-\ell_1\rangle_A |\ell_2\rangle_B) / \sqrt{2}$ is transformed by the HOM filter as follows:

$$|\Psi\rangle \xrightarrow{\text{HOM filter}} \frac{1}{2\sqrt{2}} \left(i|l_1\rangle^1 |-\ell_2\rangle^1 + i|l_1\rangle^2 |-\ell_2\rangle^2 + |l_1\rangle^1 |-\ell_2\rangle^2 - |l_1\rangle^2 |-\ell_2\rangle^1 \right) \pm \frac{1}{2\sqrt{2}} \left(i|-\ell_1\rangle^1 |\ell_2\rangle^1 + i|-\ell_1\rangle^2 |\ell_2\rangle^2 - |-\ell_1\rangle^1 |\ell_2\rangle^2 + |-\ell_1\rangle^2 |\ell_2\rangle^1 \right), \quad (6)$$

where the superscripts 1 and 2 label the output ports of the beam-splitter. One can then show that the filter transforms the states in Eq. (5) as follows:

$$|\Psi_\ell^-\rangle \xrightarrow{\text{HOM filter}} |\Psi_\ell^-\rangle^{1,2}, \quad (7)$$

$$|\Phi_\ell^\pm\rangle \xrightarrow{\text{HOM filter}} \frac{i}{2} \left(|\Phi_\ell^\pm\rangle^{1,1} + |\Phi_\ell^\pm\rangle^{2,2} \right). \quad (8)$$

Note that the antisymmetric singlet state $|\Psi_\ell^-\rangle$ exhibits anti-bunching; no two photons are in the same output port. For the two symmetric states, however, photons bunch and exit in the same port of the beam-splitter. Therefore, conditioning the photon detection on coincidence between the two output ports automatically discards the contribution of symmetric states in Eq. (5), leading to the following distillation result:

$$|\Psi_\ell\rangle \xrightarrow{\text{HOM filter}} c_0 |\Psi_\ell^-\rangle^{1,2}. \quad (9)$$

In this manner, noise arising from turbulence is converted to losses, with the probability $|c_0|^2$ representing the fraction of singlets distilled. This fraction naturally depends on the strength of turbulence: with increasing turbulence, $|c_0|$ decays to 0. Given that only anti-symmetric states exhibit anti-bunching after the HOM filter, the choice of the initial singlet state is logical and necessary, that is, because all symmetric states produce no coincidence signal after the HOM filter.³⁸ Note that the above treatment would also be valid in the case of two photons going through two turbulence screens. This is because given a weak turbulence operator \hat{M}_i acting on photon i we have, within a given OAM subspace,

$$\hat{M}_A \otimes \hat{M}_B |\Psi_\ell^-\rangle \rightarrow \tilde{c}_0 |\Psi_\ell^-\rangle + (\dots)_{\text{symmetric}}. \quad (10)$$

However, one should expect the fraction of distilled states to be even lower than in the case of one photon going through turbulence, with $|c_0| \geq |\tilde{c}_0|$.

III. EXPERIMENTAL REALISATION

We experimentally demonstrated our distillation scheme using the setup in Fig. 1(a). Pairs of entangled photons were produced through SPDC. We pumped a 3-mm type-I BBO crystal with a 355 nm laser at 350 mW average power and 80 MHz repetition rate, producing the symmetric SPDC state,

$$|\Psi\rangle_{\text{SPDC}} = \alpha_0 |0\rangle_A |0\rangle_B + \sum_{\ell>0} \alpha_\ell |\Psi_\ell^+\rangle_{AB}, \quad (11)$$

where $|\Psi_\ell^+\rangle_{AB} = (|l\rangle_A |-\ell\rangle_B + |-\ell\rangle_A |l\rangle_B) / \sqrt{2}$. Using a pair of Dove prisms (DP) in the path of photon A, we controlled the

symmetry of OAM subspaces by inducing an OAM-dependent phase in the SPDC state: $|\ell\rangle \rightarrow \exp(2i\ell\theta)|\ell\rangle$, where θ is the angle between the two Dove prisms:

$$|\Psi_\ell^+\rangle \xrightarrow{\text{DPs}} \frac{\exp(2i\ell\theta)|\ell\rangle |-\ell\rangle + \exp(-2i\ell\theta)|-\ell\rangle |\ell\rangle}{\sqrt{2}}. \quad (12)$$

For $\theta = (2n+1)\pi/4\ell$ with $n \in \mathbb{N}$, one achieves the conversion to anti-symmetric state in all the OAM subspaces. We set $\theta = \pi/4$ and obtained, up to a global phase, the following selection rules:

$$|\Psi_\ell^+\rangle \xrightarrow{\theta=\pi/4} \begin{cases} |\Psi_\ell^-\rangle & \text{for odd } \ell, \\ |\Psi_\ell^+\rangle & \text{for even } \ell. \end{cases} \quad (13)$$

Photon A then propagates through turbulence. We considered a turbulent channel with weak scintillation such that atmospheric perturbations can be summed to a unitary transformation, i.e., a single turbulence phase screen,¹⁶ and thus does not lead to a decay in purity. In our case, the turbulence phase screen was modelled based on Kolmogorov's theory and printed on a glass plate with different zones of average phase fluctuations, as shown in Fig. 1(b). In the path of photon B, we placed a delay line, consisting of a Dove prism mounted on a piezo-controlled stage, to adjust the delay in arrival time of the two photons at the BS in the HOM filter. Photons exiting the HOM filter were then analysed using spatial filters encoded on a spatial light modulator (SLM), coupled to single-mode fibres and measured in coincidence.

Initially, we calibrated the HOM filter by scanning for the characteristic dip of coincidence counts in HOM interference. The aim is to demonstrate the efficacy of the distillation scheme by performing a quantum state tomography at points of zero and maximum visibility of the HOM dip; at zero visibility, the HOM filter is in the "OFF" state (out of the HOM interference region), while at maximum visibility, it is in the "ON" state (lowest point in the HOM interference region). Using the digital holograms encoded on the SLM, we post-selected the $\ell = 0$ subspace (symmetric state) from the SPDC state and show the quantum interference signal in Fig. 2(a) in the presence and absence of turbulence. The visibility, \mathcal{V} , was computed from the coincidence counts inside (C_{in}) and outside the dip (C_{out}) as follows:

$$\mathcal{V}_{\text{dip}} = \frac{C_{\text{out}} - C_{\text{in}}}{C_{\text{out}} + C_{\text{in}}}. \quad (14)$$

We obtained, respectively, a visibility of 84.4% and 75.7% for the dip without and with turbulence. The decay in visibility that we measured can be attributed to the decay in signal-to-noise ratio resulting from turbulence-induced intermodal scattering that reduces the coincidence rates. We will show further that this does affect the distillation of singlet Bell states.

We extended the measurement of the HOM interference trace to the $\ell = \pm 1$ subspace, where the SPDC state has been made antisymmetric. This is done by projecting the photon pair on conjugate OAM states. Due to the anti-bunching effect after the HOM filter, one would expect a HOM peak rather than a dip. This is because events with two-photons in one

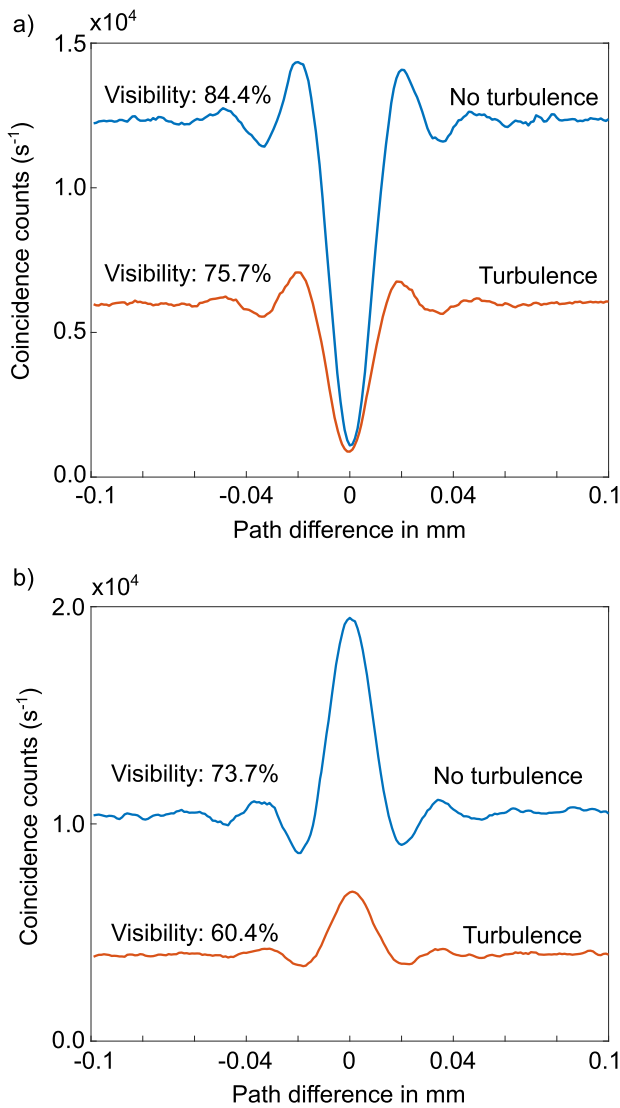


FIG. 2. Hong-Ou-Mandel interference signal for (anti)symmetric states. Delaying one photon with respect to the other leads to (a) a dip and (b) a peak in coincidence counts for the symmetric ($\ell = 0$) and antisymmetric $\ell = \pm 1$ states, respectively. In the presence of turbulence, the visibility of the HOM interference decays in both subspaces, together with the coincidence counts.

output port of the BS are in theory non-existent when the filter is in the ON state. Indeed we measured, as shown in Fig. 2(b), HOM peaks without and with turbulence with visibilities of 73.7% and 60.4%, respectively. In this case, the calculation of visibility was done differently and we will argue the formula we used.

The standard formula in Eq. (14) is adequate for fringes with an ideal minimum of zero; under this condition, the visibility is equal to unity. This is indeed the case for the HOM dip. Due to the bunching effect with the HOM filter ON, symmetric states attain, in principle, a minimum of zero coincidence

counts. Therefore the visibility of the dip can be computed as in Eq. (14). For antisymmetric states, coincidence counts should, in theory, increase two-fold when the HOM filter is in the ON state, with no zero minimum. Under Eq. (14), this would lead to negative visibility values with absolute maximum less than unity. Rather, we choose to express the visibility of the HOM peak as follows:

$$\mathcal{V}_{\text{peak}} = \frac{C_{\text{out}} - (2C_{\text{out}} - C_{\text{in}})}{C_{\text{out}} + (2C_{\text{out}} - C_{\text{in}})} = \frac{-C_{\text{out}} + C_{\text{in}}}{3C_{\text{out}} - C_{\text{in}}}. \quad (15)$$

This way of computing the visibility effectively inverts the HOM trace about the minimum (HOM filter OFF), turning the HOM peak into a HOM dip with zero absolute minimum, whose visibility can be calculated as in Eq. (14). Assume a minimum of 1 for the HOM peak signal ($C_{\text{out}} = 1$). Switching the HOM filter to the ON state leads to a maximum coincidence signal of 2 ($C_{\text{in}} = 2$), resulting in a maximum visibility of $\mathcal{V}_{\text{peak}} = 1$.

Having established the reference point for the HOM filter (determination of the dip/peak position), we demonstrated the effectiveness of the distillation process by performing a quantum state tomography of the two-photon state with the HOM filter OFF/ON. Figure 3(a) graphically depicts the joint projective measurements performed within the $\ell = \pm 1$ OAM subspace to realise an over-complete quantum state tomography⁴⁰ with the HOM filter in the OFF state. We selected 6 different locations on the surface of the turbulence plate to implement our distillation scheme. The choice of location was solely guided by our need to cover a range of turbulence conditions. With the HOM filter still in the OFF state, we performed a tomography of the two-photon state at the six different locations, as shown in Fig. 3(b). As expected, the measurement outcomes wildly deviate in the presence of turbulence. We then repeated the measurement with the HOM filter in the ON state. Observe that with respect to the reference shown in Fig. 3(c), the tomographic measurements at the previous 6 locations [Fig. 3(d)] are qualitatively similar, indicating that the HOM filter is indeed distilling maximally entangled states.

To each of these tomographic measurements, we can attach a quantitative measure to numerically demonstrate the efficacy of the HOM filter. Our figure of merit here is the fidelity, F , of the reconstructed two-photon density matrix ρ , with respect to the maximally entangled singlet state $\rho_T = |\Psi_{\ell}^{-}\rangle\langle\Psi_{\ell}^{-}|$,

$$F = \text{tr}\left(\sqrt{\sqrt{\rho_T}\rho\sqrt{\rho_T}}\right)^2 = \langle\Psi_{\ell}^{-}|\rho|\Psi_{\ell}^{-}\rangle. \quad (16)$$

For each of the reference measurements in Figs. 3(a) and 3(c), the measured fidelity was in excess of 99%.

When post-selecting the antisymmetric space $\ell = \pm 1$, we show that with the HOM filter OFF, the fidelity with respect to the maximally entangled singlet state decays, as shown in Fig. 4(a), from 0.90 down to 0.095. However, with the HOM filter ON, the fidelity remains constant with $F > 0.85$ and consistently above the results with the filter OFF. We performed a similar set of measurements with the next antisymmetric subspace $\ell = \pm 3$. States within this subspace are more resilient

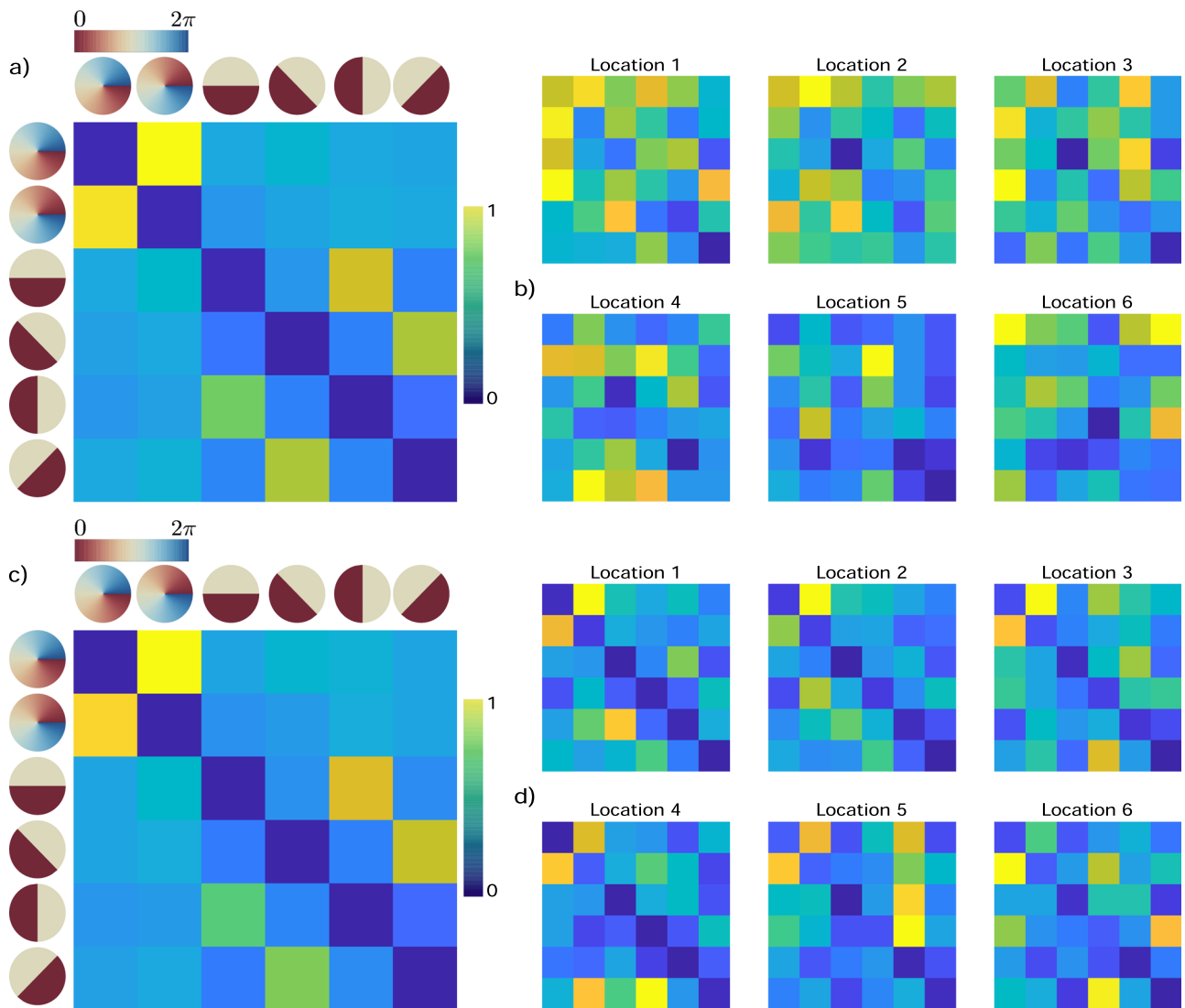


FIG. 3. Quantum state tomography of two-photon states with the HOM filter OFF/ON. (a) shows the normalised tomographic measurement performed with the HOM filter OFF in the absence of turbulence. (b) We introduced the turbulence plate in the path of photon A and show the effect of turbulence on the state tomography measurement outcomes. We repeated the measurements, this time with the HOM filter ON (c) in the absence of turbulence and (d) for the same locations across the turbulence plate.

to turbulence due to their larger separation in OAM space.²³ Using the same locations as before yielded relatively high fidelities without any significant spread. Therefore we chose another set of locations across the turbulence phase plate (TPP) and compared the results with the HOM filter OFF and ON, as shown in Fig. 4(b). Similar to the previous case, with the HOM filter OFF, we measured a decay of fidelity from 0.95 down to 0.032. When switching the filter to the ON state, the fidelity remained consistently high for the various locations, with $F > 0.90$.

The distillation scheme we have demonstrated enables current and future quantum technologies. Turbulence makes

it impractical to employ spatial modes for long distance quantum communication, with the measurement fidelity decaying with increasing turbulence. Our scheme enables one to recover, with high fidelity, information that would have otherwise been lost. The resilience of our scheme to a range of turbulence would enable the distribution of photon pairs over significant distances through turbulence. This could be envisaged in a network configuration, where photon pairs are prepared at location A and sent to a remote location B. Upon arrival at location B, photon pairs in the singlet states are distilled, before partaking in other quantum processes that include quantum computation and communication.

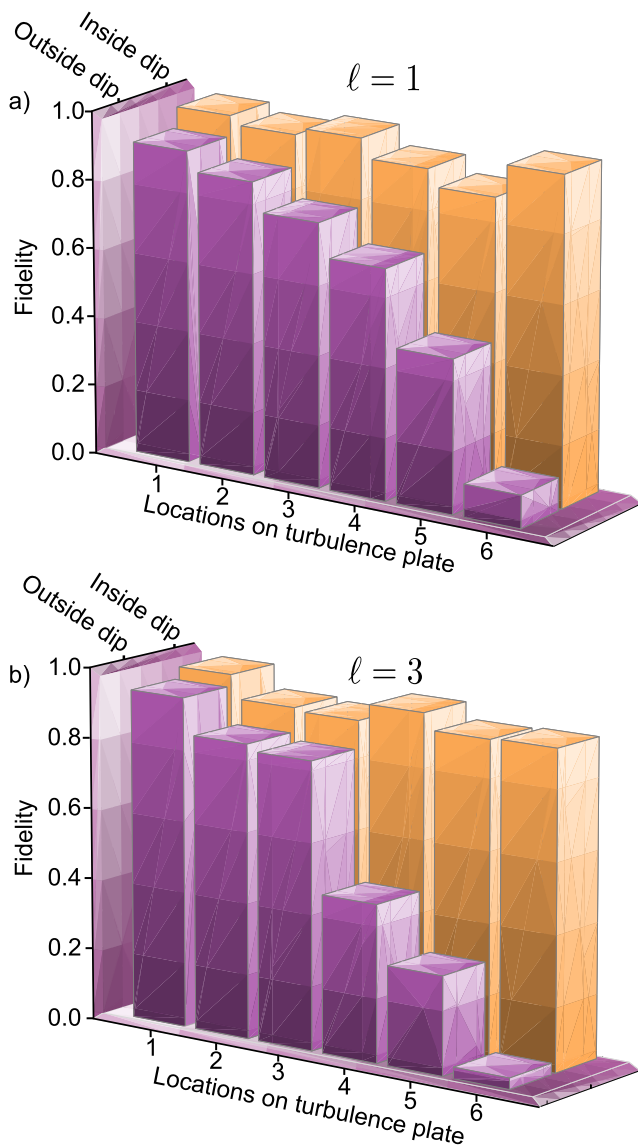


FIG. 4. Distillation of singlet states. With the HOM filter in the OFF state (outside the dip), the fidelity of the measured state with respect to the singlet Bell state decays with increasing perturbations of the turbulence phase plate. Switching the filter to the ON state results in the distillation of states with high-fidelity with respect to the singlet Bell state. This is shown within the (a) $\ell = \pm 1$ and (b) $\ell = \pm 3$ subspaces.

Furthermore, high-fidelity entangled states are critical resources to build a quantum repeater, a fundamental building block of quantum networks.⁹ Our distillation scheme can be readily implemented with current technologies.

IV. CONCLUSION

We have demonstrated an entanglement distillation scheme based on quantum interference of two entangled

photons. The distillation process is realised by using a Hong-Ou-Mandel filter that causes symmetric and antisymmetric Bell states to respectively bunch and anti-bunch upon exiting the filter through a 50:50 beam-splitter. By conditioning the detection system on coincidence between the output ports of the HOM filter, we have shown theoretically and experimentally the distillation of antisymmetric singlet states. The entanglement concentration process was tested for a coherent superposition of symmetric and antisymmetric states, produced by perturbing a singlet state with a one-sided weak turbulent channel. We have illustrated our distillation scheme by filtering OAM singlets carrying $\ell = \pm \hbar$ and $\ell = \pm 3\hbar$ quanta of OAM from an ensemble of non-maximally entangled pure states. When compared to a singlet Bell state, we have experimentally demonstrated the distillation of states with average fidelity higher than 90% from an ensemble with average fidelity as low as 3%. The states distilled can reliably be used further in other quantum processes.

REFERENCES

- S.-K. Liao, W.-Q. Cai, W.-Y. Liu, L. Zhang, Y. Li, J.-G. Ren, J. Yin, Q. Shen, Y. Cao, Z.-P. Li, F.-Z. Li, X.-W. Chen, L.-H. Sun, J.-J. Jia, J.-C. Wu, X.-J. Jiang, J.-F. Wang, Y.-M. Huang, Q. Wang, Y.-L. Zhou, L. Deng, T. Xi, L. Ma, T. Hu, Q. Zhang, Y.-A. Chen, N.-L. Liu, X.-B. Wang, Z.-C. Zhu, C.-Y. Lu, R. Shu, C.-Z. Peng, J.-Y. Wang, and J.-W. Pan, "Satellite-to-ground quantum key distribution," *Nature* **549**, 43 (2017).
- J.-G. Ren, P. Xu, H.-L. Yong, L. Zhang, S.-K. Liao, J. Yin, W.-Y. Liu, W.-Q. Cai, M. Yang, L. Li, K.-X. Yang, X. Han, Y.-Q. Yao, J. Li, H.-Y. Wu, S. Wan, L. Liu, D.-Q. Liu, Y.-W. Kuang, Z.-P. He, P. Shang, C. Guo, R.-H. Zheng, K. Tian, Z.-C. Zhu, N.-L. Liu, C.-Y. Lu, R. Shu, Y.-A. Chen, C.-Z. Peng, J.-Y. Wang, and J.-W. Pan, "Ground-to-satellite quantum teleportation," *Nature* **549**, 70 (2017).
- J. Yin, Y. Cao, Y.-H. Li, S.-K. Liao, L. Zhang, J.-G. Ren, W.-Q. Cai, W.-Y. Liu, B. Li, H. Dai, G.-B. Li, Q.-M. Lu, Y.-H. Gong, Y. Xu, S.-L. Li, F.-Z. Li, Y.-Y. Yin, Z.-Q. Jiang, M. Li, J.-J. Jia, G. Ren, D. He, Y.-L. Zhou, X.-X. Zhang, N. Wang, X. Chang, Z.-C. Zhu, N.-L. Liu, Y.-A. Chen, C.-Y. Lu, R. Shu, C.-Z. Peng, J.-Y. Wang, and J.-W. Pan, "Satellite-based entanglement distribution over 1200 kilometers," *Science* **356**, 1140 (2017).
- V. Giovannetti, S. Lloyd, and L. MacCone, "Advances in quantum metrology," *Nat. Photonics* **5**, 222 (2011).
- V. Giovannetti, S. Lloyd, and L. MacCone, "Quantum-enhanced measurements: Beating the standard quantum limit," *Science* **306**, 1330 (2004).
- P. Kómár, E. M. Kessler, M. Bishof, L. Jiang, A. S. Sørensen, J. Ye, and M. D. Lukin, "A quantum network of clocks," *Nat. Phys.* **10**, 582 (2014).
- J. I. Cirac, A. K. Ekert, S. F. Huelga, and C. Macchiavello, "Distributed quantum computation over noisy channels," *Phys. Rev. A* **59**, 4249 (1999).
- L. Jiang, J. M. Taylor, K. Nemoto, W. J. Munro, R. Van Meter, and M. D. Lukin, "Quantum repeater with encoding," *Phys. Rev. A* **79**, 032325 (2009).
- H. J. Kimble, "The quantum internet," *Nature* **453**, 1023-1030 (2008).
- J. L. O'Brien, "Optical quantum computing," *Science* **318**, 1567 (2007).
- N. Gisin and R. Thew, "Quantum communication," *Nat. Photonics* **1**, 165 (2007).
- A. Mair, A. Vaziri, G. Weihs, and A. Zeilinger, "Entanglement of the orbital angular momentum states of photons," *Nature* **412**, 313 (2001).
- M. Krenn, M. Malik, M. Erhard, and A. Zeilinger, "Orbital angular momentum of photons and the entanglement of Laguerre-Gaussian modes," *Philos. Trans. R. Soc., A* **375**, 20150442 (2017).
- M. Erhard, R. Fickler, M. Krenn, and A. Zeilinger, "Twisted photons: New quantum perspectives in high dimensions," *Light: Sci. Appl.* **7**, 17146 (2018).
- A. C. Dada, J. Leach, G. S. Buller, M. J. Padgett, and E. Andersson, "Experimental high-dimensional two-photon entanglement and violations of generalized Bell inequalities," *Nat. Phys.* **7**, 677 (2011).

- ¹⁶A. Hamadou Ibrahim, F. S. Roux, M. McLaren, T. Konrad, and A. Forbes, "Orbital-angular-momentum entanglement in turbulence," *Phys. Rev. A* **88**, 012312 (2013).
- ¹⁷Y. Zhang, S. Prabhakar, A. H. Ibrahim, F. S. Roux, A. Forbes, and T. Konrad, "Experimentally observed decay of high-dimensional entanglement through turbulence," *Phys. Rev. A* **94**, 032310 (2016).
- ¹⁸C. Gopaul and R. Andrews, "The effect of atmospheric turbulence on entangled orbital angular momentum states," *New J. Phys.* **9**, 94 (2007).
- ¹⁹F. S. Roux, T. Wellens, and V. N. Shatokhin, "Entanglement evolution of twisted photons in strong atmospheric turbulence," *Phys. Rev. A* **92**, 012326 (2015).
- ²⁰B.-J. Pors, C. H. Monken, E. R. Eliel, and J. P. Woerdman, "Transport of orbital-angular-momentum entanglement through a turbulent atmosphere," *Opt. Express* **19**, 6671–6683 (2011).
- ²¹H. Avetisyan and C. H. Monken, "Mode analysis of higher-order transverse-mode correlation beams in a turbulent atmosphere," *Opt. Lett.* **42**, 101–104 (2017).
- ²²S. K. Goyal, A. H. Ibrahim, F. S. Roux, T. Konrad, and A. Forbes, "The effect of turbulence on entanglement-based free-space quantum key distribution with photonic orbital angular momentum," *J. Opt.* **18**, 064002 (2016).
- ²³M. Malik, M. O'Sullivan, B. Rodenburg, M. Mirhosseini, J. Leach, M. P. J. Lavery, M. J. Padgett, and R. W. Boyd, "Influence of atmospheric turbulence on optical communications using orbital angular momentum for encoding," *Opt. Express* **20**, 13195 (2012).
- ²⁴M. V. da Cunha Pereira, L. A. P. Filpi, and C. H. Monken, "Cancellation of atmospheric turbulence effects in entangled two-photon beams," *Phys. Rev. A* **88**, 053836 (2013).
- ²⁵C. H. Bennett, H. J. Bernstein, S. Popescu, and B. Schumacher, "Concentrating partial entanglement by local operations," *Phys. Rev. A* **53**, 2046 (1996).
- ²⁶R. T. Thew and W. J. Munro, "Entanglement manipulation and concentration," *Phys. Rev. A* **63**, 030302 (2001).
- ²⁷N. A. Peters, J. B. Altepeter, D. Branning, E. R. Jeffrey, T.-C. Wei, and P. G. Kwiat, "Erratum: Maximally entangled mixed states: Creation and concentration [Phys. Rev. Lett. 92, 133601 (2004)]," *Phys. Rev. Lett.* **96**, 159901 (2006).
- ²⁸P. G. Kwiat, S. Barraza-Lopez, A. Stefanov, and N. Gisin, "Experimental entanglement distillation and 'hidden' non-locality," *Nature* **409**, 1014 (2001).
- ²⁹S. Bose, V. Vedral, and P. L. Knight, "Purification via entanglement swapping and conserved entanglement," *Phys. Rev. A* **60**, 194 (1999).
- ³⁰Z. Zhao, J.-W. Pan, and M. S. Zhan, "Practical scheme for entanglement concentration," *Phys. Rev. A* **64**, 014301 (2001).
- ³¹Z. Zhao, T. Yang, Y.-A. Chen, A.-N. Zhang, and J.-W. Pan, "Experimental realization of entanglement concentration and a quantum repeater," *Phys. Rev. Lett.* **90**, 207901 (2003).
- ³²T. Yamamoto, M. Koashi, Ş. K. Özdemir, and N. Imoto, "Experimental extraction of an entangled photon pair from two identically decohered pairs," *Nature* **421**, 343 (2003).
- ³³J.-W. Pan, S. Gasparoni, R. Ursin, G. Weihs, and A. Zeilinger, "Experimental entanglement purification of arbitrary unknown states," *Nature* **423**, 417 (2003).
- ³⁴C. K. Hong, Z. Y. Ou, and L. Mandel, "Measurement of subpicosecond time intervals between two photons by interference," *Phys. Rev. Lett.* **59**, 2044 (1987).
- ³⁵Y. Zhang, S. Prabhakar, C. Rosales-Guzmán, F. S. Roux, E. Karimi, and A. Forbes, "Hong-Ou-Mandel interference of entangled Hermite-Gauss modes," *Phys. Rev. A* **94**, 033855 (2016).
- ³⁶Y. Zhang, F. S. Roux, T. Konrad, M. Agnew, J. Leach, and A. Forbes, "Engineering two-photon high-dimensional states through quantum interference," *Sci. Adv.* **2**, e1501165 (2016).
- ³⁷Y. Zhang, M. Agnew, T. Roger, F. S. Roux, T. Konrad, D. Faccio, J. Leach, and A. Forbes, "Simultaneous entanglement swapping of multiple orbital angular momentum states of light," *Nat. Commun.* **8**, 632 (2017).
- ³⁸S. Prabhakar, C. Mabena, T. Konrad, and F. S. Roux, "Turbulence and the Hong-Ou-Mandel effect," *Phys. Rev. A* **97**, 013835 (2018).
- ³⁹M. J. Padgett and J. Courtial, "Poincaré-sphere equivalent for light beams containing orbital angular momentum," *Opt. Lett.* **24**, 430 (1999).
- ⁴⁰B. Jack, J. Leach, H. Ritsch, S. M. Barnett, M. J. Padgett, and S. Franke-Arnold, "Precise quantum tomography of photon pairs with entangled orbital angular momentum," *New J. Phys.* **11**, 103024 (2009).